Prevention of cold cracking in ASTM A516 Gr. 70 steel weldment

M.A. Morsy[1], A. Mahdy[2], and M. A, Al-Hameed[3]

[1.]Researcher, CMRDI, Cairo. Egypt
[2.] Professor Assistant. Faculty of Engineering, Al-Azhar university, Egypt.
[3.] Engineer, Petroget Company.
Morsy_abokhala@yahoo.com

Abstract: Cold cracking susceptibility was studied in welding of ASTM A516 Gr. 70 steel using AWS A5.1 E7018 electrode. Y- Tekken cracking test was applied to study the effect of preheating and heat input on cracking index. Application of preheating temperature of 150^0C resulted in a disappearance of cracks. Also, increasing the heat input from 0.89 kJ/mm to 1.34 kJ/mm significantly decreasing the cracking index. Increasing the drying temperature of covered electrode has a significant effect on decreasing the diffusible hydrogen content. Cold crack started at the HAZ root (Martensitic structure) and propagated through the fusion line to the weld metal. Fracture surface observation by SEM indicating transgranular cleavage fracture at the fusion line (HAZ), quasi cleavage fracture at the transition zone ahead of fusion line and a ductile fracture at the weld metal.

1. Introduction

Hydrogen induced cracking (also referred to as cold cracking and delayed cracking) is the most serious problem affecting weldability of hardenable steels. This type of cracking result from the combined effect of three factors which are susceptible (brittle) microstructure, presence of diffusible hydrogen in weld metal and the residual stress [1-10].

For lower hardenability steel, a hardness control method is used to control the welding conditions that can give cooling rates slow enough to avoid brittle micro structure in the heat affected zone (HAZ). For high hydrogen-consumables, this critical hardness value is 350 Hv, while for low hydrogen consumables (< 10ml / 100 gm. weld metal) it increase to 400 Hv. For high hardenability steel, a hydrogen control method is used..Even slow cooling rates cannot prevent the formation of hard, brittle microstructure [11].

Yurioka *et al.* [12] studied the effect of preheating temperature to avoid cold cracking. They proposed a new carbon equivalent equation to avoid cold cracking.

SEO *et al.* [13] studied the effect of weld microstructure on cold cracking susceptibility of FCAW weld metals. They identify the quantified parameter for weld microstructure with respect to weld metal cold cracking.

Gedeon *et al.* [14] studied the fracture modes of high strength steel welds as a function of the stress intensity and hydrogen content at the cracking zone in implant tested welds. They concluded that large amount of hydrogen increased the intergranular fracture mode rather than microvoid coalescence.

Magudeeswaran *et al.* [15] investigated the weldability of armour grade high strength, quenched and tempered steel weldments. They described that the use of austenitic stainless steel filler metal has a high resistance to hydrogen induced cracking compared with other welds.

ASTM A 516 Grade 70 Steel is a special high strength Normalized C-Mn Steel for boiler and pressure vessel application. It is highly recommended in oil, gas and petrochemical industry. Although its carbon equivalent is low, it suffer from cold cracking after welding that increases the demands to study the effect of welding variables on cold cracking susceptibility of this steel.

The aim of the preset work is to study the effect of welding variable such as heat input, application of preheating temperature, and weld metal diffusible hydrogen content on cold cracking tendency. Microstructure of weld metal and HAZ microstructure, hardness distribution and SEM observations of the fracture surface was investigated to give better insight into the mechanism of cold cracking in ASTM A 516 Gr 70 steel.

2. Experimental work
2.1. Material

ASTM A516 Gr. 70 steel with a thickness of 25 mm is used to study its cold crack susceptibility.

SMAW electrode of AWS A5.1 E7018 with diameter of 3.2mm is used as a filler metal.

The welding parameters are shown Table1.

Table 1. Welding parameters

Electrode	Current, A	Voltage, V	Speed, mm/min160	Heat input, kI/mm
E7018	100	28	160	0.89
E7018	150	28	160	1.34

The heat input is calculated by using the following equation:

$$E = \eta X \frac{60VA}{s} X 10^{-3}$$

E, η, V, A and S represent,respectively, the heat input (kJ/mm), arc efficiency (about 0.85 for shielded metal arc welding), the voltage (V), current (A) and welding speed (mm/min).

2.2. Cold cracking test

Cold cracking test was performed using JIS Z 3158. After 48 hours of welding of test bead, the weld bead is examined to detect the cracks on the surface and also at the cross sections. Cracking index was calculated as described in JIS Z 3158 slandered.

2.3. Diffusible hydrogen test

The hydrogen glycerin displacement method is applied according to JIS Z 3113.

2.4. Macrostructure and microstructure of cracking test Specimens

The cross section of the test region was prepared by using cooling disc and was ground through grit silicon papers (from 180-1000). Finally polishing was conducted using 0.5 µm alumina past, then cleaned and dried. The macrostructure was revealed using 5% Nital Solution as etchant and observed using stereoscope. The microstructure was observed using optical microscope after the polished specimen was etched by 2% Nital solution. Hardness distribution was determined using DVK-2 Matsuzawa Vickers hardness testing device at a load of 20 kg for 15 second loading time and a load speed of 70 µm/s.

3 Results and Discussion

3.1-Metallurgical and mechanical properties of ASTM A516 Gr 70 steel

The chemical composition and tensile properties of base metal are shown in Tables 1 and 2 respectively.

Table 1 Chemical composition of base metal, Wt%

Steel type	C	Si	Mn	P	S	Fe	Ceq*
ASTM A 516 Gr 70	0.187	0.318	1.12	0.012	0.007	Bal.	0.39

*Carbon equivalent (Ceq)= C + (Mn/6) + (Si/24)

Table 2 Tensile properties of base metal

Steel type	Ultimate tensile stress, N/mm²	Yield stress, N/mm²	Elongation, %
ASTM A 516 Gr. 70	315	499.4	29.5

From the calculation of carbon equivalent, the steel has a moderate carbon equivalent. The strength and elongation percentage is conforming to that of the standard values.

The microstructure of ASTM A516 Gr 70 steel is shown in Fig.1. It is ferrite –pearlite structure.
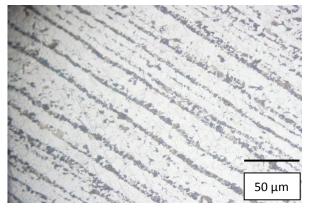

50 µm

Fig. 1 Microstructure of ASTM A516 Gr 70 steel

3.2 Effect of drying temperature of covered electrode on its diffusible hydrogen content

Figure 2 shows the effect of drying temperature on the weld metal diffusible hydrogen content using AWS A5.1 E7018 electrode. The increase in drying temperature resulted in a significant decrease in weld metal diffusible hydrogen content. The increase in drying temperature resulted in the increase in the removal of electrode covering moisture content which is the source of weld diffusible hydrogen potential.

3.3- Cold Cracking Susceptibility Results

Cold cracking test was conducted using AWS A5.1 E7018 Electrode (H_d = 15ml/100gm weld metal without drying and H_d = 7.5ml/100gm weld metal after drying at 300 °C for 2 hours). The cracking index is shown in Fig 3. Using of electrode without drying resulted in a formation of cracks with cracking index of 82.5 %. However, using the same electrode

after drying at 300 °C for 2 hours resulted in a reduction of cracking index to 50%.
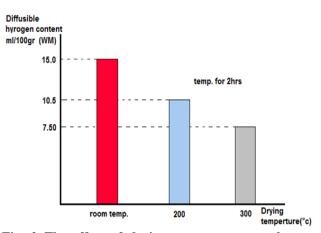

Fig. 2 The effect of drying temperature on the diffusible hydrogen content

A preheating temperature of 150 °C was applied to the cracking test specimen before welding. Application of preheating temperature of 150 °C and using electrode that was dried at 300 °C for 2 hours resulted in a disappearance of cold cracks (cracking

Index=0). On the other hand, preheating application temperature of 150 °C and using of covered electrode without drying resulted in a formation of cracks with cracking index of 65 %.

Figure 4 show some examples of cross sections of the cold cracking test using different condition of preheating and drying condition of covered electrode.
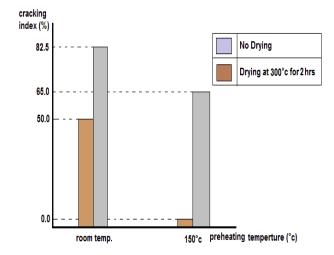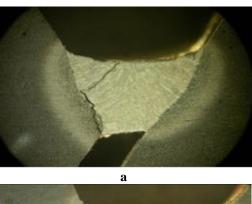

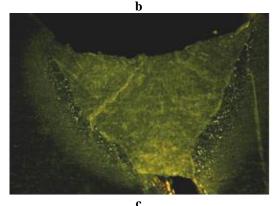Fig. 3 Effect of preheating temperature on cold cracking index

a

b

c

d

Fig. 4 Macrostructures of the cross sections of cold cracking test using a) Welding without drying, b) Welding with drying at 300 ^{0}C for 2 hours, c) Welding without drying and preheating at 150 ^{0}C and d) Welding with drying at 300 ^{0}C for 2 hours and preheating at 150 ^{0}C

The increase in heat input from 0.89 kJ/ mm to 1.34 kJ/ mm through the increase in welding current from 100 A to 150 A in welding with drying electrodes at 300 ^{0}C for 2 hours and without preheating resulted in a disappearance of cold cracks as shown in Figs. 5 and 6. On the other hand, the increase of heat input without drying the electrode resulted in a decrease in the cracking index from 85.5 to 72% as shown in Fig.5.
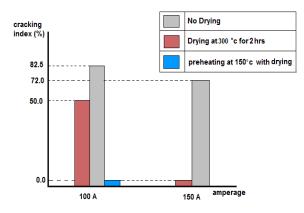

Fig. 5 Effect of heat input on cracking index at different electrode conditions, welding current and preheating temperature
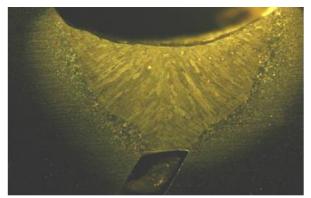

Fig. 6 Macrostructure of the cross section of the test welded using a welding current of 150A with electrode dried at 300 ^{0}C for 2 hours and without preheating

3.4-Microstructure of weld metal and heat affected zone of the cracking test specimens

Microstructure of the weld metal of the cold cracking test spacemen welded using AWS A5.1 E7018 electrode is shown in Fig.7. It is a columnar structure containing acicular ferrite (AF) with some grain boundary ferrite (GBP).

Fig. 7 Microstructure of the weld metal using AWS A5.1 E7018 electrode

Figure 8 shows the microstructure at the heat affected zone (HAZ) which is a martensitic structure (at the grain coarsening zone).

Fig. 8 microstructure at the heat affected zone (HAZ)

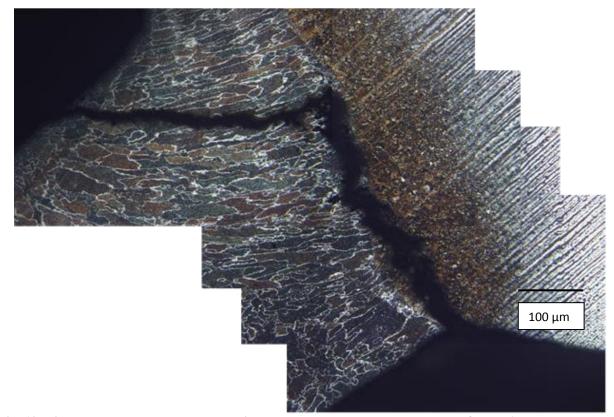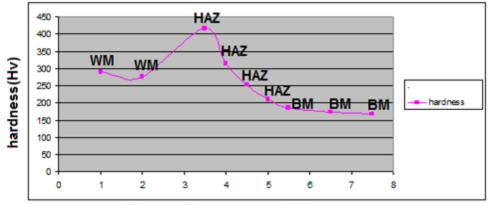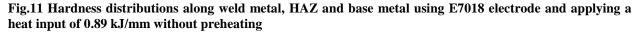**Fig. 9 Microstructure at the cracked HAZ**

Fig. 10 Microstructure at the cracked specimen where crack started at the root of the HAZ and propagated through HAZ and weld metal and finally terminated at the surface of weld metal.

Figure 9 shows the microstructure at the cracked heat affected zone (HAZ) which show that the structure is martensitic structure.

Most of cracks were observed at the heat affected zone and propagated through the fusion line to the weld metal as shown in Fig.10 (see also the macrostructures of the cracked specimens in Figs. 4 a, b and c). It is started at the root of the HAZ (fusion line) and propagated in the HAZ and weld metal and terminated at the weld surface as shown in Fig10.

Fig.11 Hardness distributions along weld metal, HAZ and base metal using E7018 electrode and applying a heat input of 0.89 kJ/mm without preheating

Stress concentration in generally higher at the root than at the toe [16-18]. This accentuates the appearance of root cracking at the expense of toe cracking [17].

3.5- Hardness distribution at the weld metal and heat affected zone

The hardiness distribution at the weld metal, HAZ and base metal in the specimen welded using E7018 Electrode without preheating and applying a heat input of 0.89 kJ/mm is shown in Fig 11.
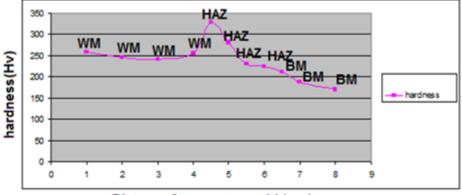
Hardness at the heat affected zone show a maximum value of 420 HV. The average hardness value at the weld metal is about 280 HV.

Application of 150 ^{0}C resulted in a significant decrease in the maximum hardness at the heat affected zone to about 325 HV as shown in Fig 12. The average hardness at the weld metal decreased to about 250 HV.

Application of the preheating with the application of low diffusible hydrogen content resulted in a significant reduction in the cold cracking index (cracking index=0). This could be attributed 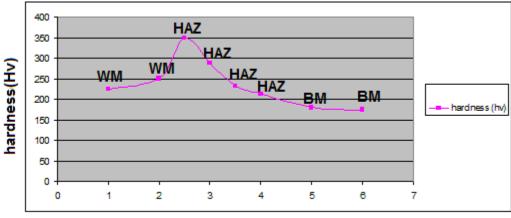to the delay of the rate of cooling in the HAZ and a subsequent reduction in hardness of its martensitic structure as shown in Fig. 12. Also, preheating accelerates hydrogen removal and decrease the residual stress [12]. This reflect the disappearance of cold cracking (crack index = 0) at the preheated test specimen as shown in Figs. 3 and 4.

The increase in the heat input to 1.34 kJ/mm through the increase in welding current from 100 to 150 A resulted in a decrease in the maximum hardness at the heat affected zone to 350 HV and a decrease in the average hardness at the weld metal to about 245 HV as shown in Fig. 13. Thus, the increase in the heat input resulted in a significant delay in the rate of cooling of the HAZ and a subsequent reduction in its hardness values. This also reflect the disappearance of cracks with the increase in heat input as shown in Figs. 5 and 6.

Fig, 12 Hardness distributions along weld metal, HAZ and base metal using E7018 electrode and applying a heat input of 0.89 kJ/mm with preheating temperature of 150 ^{0}C

Fig. 13 Hardness distributions along weld metal, HAZ and base metal using E7018 electrode and applying a heat input of 1.34 kJ/mm without preheating
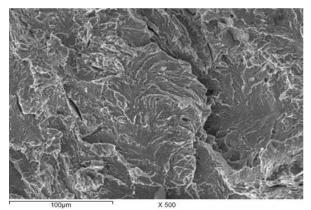
3.6 Fracture surface

Fig. 14 SEM observation of the fracture surface of cold cracked specimen at HAZ
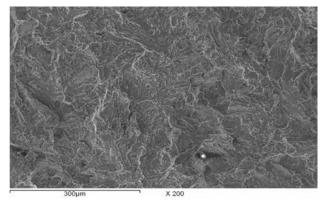

Fig. 15 SEM observation of the fracture surface of cold cracked specimen at the transition between the weld metal and HAZ
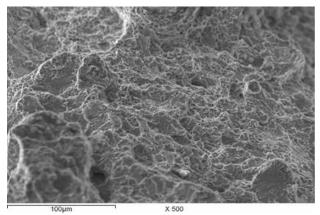

Fig. 16 SEM observation of the fracture surface of cold cracked specimen at the weld metal

SEM observation of the fracture surface of cold cracking specimen at the fusion line, at the transition zone between fusion line and weld metal and at the weld metal are shown in Figs. 14.,15 and16 respectively. At the fusion line (heat affected zone) (Fig. 14), the fracture surface is a transgranular cleavage fracture (brittle fracture) surrounded by nets of dimple strips, corresponding to the size of prior austenitic grains. The cleavage regions in the fusion line indicated the presence of high embrittlement due to the increase in the hardness values as shown in Fig. 11. The fracture surface at the transition zone ahead of fusion line showed quasi-cleavage morphology as shown in Fig. 15. Inside sub-grain region, there are several cleavage facets with small parallel tear ridges as shown in Fig. 15. The tear ridges inside indicate that the cracks were initiated inside the sub-grains at the interface between ferrite matrix and cementite particles. The mixed quasi-cleavage and ductile mode in this region confirming the absence of severe embrittlement. On the other hand, the fracture surface at the weld metal shows ductile dimpled fracture mode as shown in Fig. 16. The strong effect of lath structures and low hardness of the weld metal minimize the deterioration effect of diffusible hydrogen. The presence of acicular ferrite in the weld metal (Fig.7) prohibiting the propagation of cracks initiated within the grains.

On the other hand, a ductile fracture is observed with a dimples at the weld metal as shown in Fig. 16. The existence of acicular ferrite in the weld metal (Fig. 7) increases its ductility.

Conclusion

Cold cracking susceptibility was studied in welding of ASTM A516 Gr. 70 steel using AWS 5.1 E7018 electrode. Y- Tekken cracking test was applied to study the effect of preheating and heat input on cracking index. The following results were obtained:

1. Increasing the drying temperature of covered electrode has a significant effect on decreasing the diffusible hydrogen content.

2. Application of preheating temperature of 150^0C resulted in a disappearance of cracks. Also, increasing the heat input from 0.89 kJ/mm to 1.34 kJ/mm significantly decreasing the cracking index. Martensitic structure was observed at the heat affected zone. Application of preheating temperature and increasing the heat input resulted in a decrease in the hardness of the HAZ.

3. Cold crack started at the HAZ (fusion line) root and propagated through the fusion line to the weld metal.

4. Fracture surface observation by SEM indicating transgranular cleavage fracture at the HAZ (fusion line), quasi cleavage fracture at the transition zone ahead of the fusion line and a ductile fracture at the weld metal.

References

1. Okuda N, Nishikawa Y, Aoki T, Goto A & Abe T: 'Hydrogen-induced cracking susceptibility of weld metal'. *IIW-Doc. II-1072-86 / II-A- -86*. Kobe Steel Ltd./The International Institu te of Welding, Japan, 1986. 16 p.

2. Okuda N, Ogata Y, Nishikawa Y, Aoki T, Goto A & Abe T: 'Hydrogen-induced cracking susceptibility in high-strength weld metal'. *Welding Journal* 66 (1987): May, pp. 141-s – 146-s.

3. Yatake T & Yurioka N: 'Studies of delayed cracking in steel weldments (Report 3)'. *Journal of the Japan Welding Society (JWS)* 50 (1981) 3, pp. 291–296.

4. Suzuki H & Yurioka N: 'Prevention against cold cracking in welding steels'. *Australian Welding Journal* 27 (1982) 1: Autumn 1982. Pp. 9–27.

5. Nevasmaa P & Karppi R: 'Implications on controlling factors affecting weld metal hydrogen cold-cracking in high-strength shielded-metal arc (SMAW) multipass welds'. *Report AVAL64-011043: WM-HICC VTT/3. IIW-Doc. IX-1997-01*. VTT Manufacturing Technology, Espoo 2001. 94 p. + Apps 26 p.

6. Nevasmaa P: 'Controlling factors influencing hydrogen cold cracking in high-strength multipass weld metals – Statu s Review report'. *Report VAL A:WM-HICC VTT/1*. VTT Manufacturing Technology, Espoo 2000. 51 p. + Apps 4 p.

7. Nevasmaa P, Kantanen M-S & Pan L: 'Hydrogen cold-cracking in high-strength shielded-metal arc (SMAW) multipass weld metals: experimental findings'. *Report AVAL64-001029:WM-HICC VTT/2*. VTT Manufacturing Technology, Espoo 2000. 66 p. + Apps 23 p.

8. Nevasmaa P: 'Controlling factors affecting hydrogen cold-cracking in high-strength multipass weld metals: comparison of the cracking test results between SMAW and SAW welds'. *IIW-Doc. No IX-2027-02*. VTT Industrial Systems, Espoo 2002. 46 p. + Apps 14 p.

9. Pargeter RJ: 'Effects of arc energy, plate thickness and preheat on C-Mn steel weld metal hydrogen cracking'. *TWI Research Report (CRP) No. 461/1992*. The Welding Institute, UK, November 1992.

10. Kinsey A.J: 'Weld metal hydrogen cracking during welding 450 N/mm2 yield strength steel using tubular cored electrodes'. *TWI Research Report (CRP) No. 655/1998*. The Welding Institute, UK, October 1998. 24 p.

11. Yurioka N: 'Test results of cold cracking in multi-pass weld metal'. *IIW-Doc. IX-1903-98*. Nippon Steel Corporation, The International Institute of Welding, Japan, 1998. 11 p.

12. Yurioka N., Suzuki H., Ohshita S. and Saito S. "Determination of necessary preheating temperature in steel welding" Welding journal, June, 1983, 147s-153s.

13. Seo J.S., Kim H. J. and Ryoo H.S. "Microstructural parameter controlling weld metal cold cracking" journal of achievements in materials and manufacturing engineering, April 2008, 199-202.

14. Gedeon S.A. and Eagar T.W." Assessing hydrogen -assisted cracking- Fracture modes in high strength steel weldments" June 1990, 213s-220s.

15. Magudeeswaran G., Balasubramanian V. and Madusudhan Reddy G. " Hydrogen induced cold cracking studies on armour grade high strength, quenched and tempered steel weldments" International journal of hydrogen energy, March, 2008, 1897-1908.

16. Karppi R, Ruusila J, Toyoda M, Satoh K & Vartiainen K: 'Predicting safe welding conditions with hydrogen cracking parameters'. *Scandinavian Journal of Metallurgy* 13 (1984), pp. 66–74

17. Karppi R: 'A stress field parameter for weld hydrogen cracking'. *VTT Publications 9*. Technical Research Centre of Fin land, Espoo 1982. 119 p.

18. Terasaki T, Karppi R & Satoh K: 'Relationship between critical stress of HAZ cracking and residual diffusible hydrogen content'. *Transactions of the Japan Welding Society* 10 (1979) 1, pp. 53–57.

4/26/2014